CHINESE OPTICS LETTERS

Vol. 22, No. 1 | January 2024

Dual-mode stabilization for laser to radio-frequency locking by using a single-sideband modulation and a Fabry–Pérot cavity

Yibo Wang (王一博)[1,2], Hongwei Zhang (张洪炜)[1,2], Chenhao Zhao (赵晨皓)[1,2], Gang Zhao (赵 刚)[1,2*], Xiaojuan Yan (闫晓娟)[1,2], and Weiguang Ma (马维光)[1,2**]

[1] State Key Laboratory of Quantum Optics & Quantum Optics Devices, Institute of Laser Spectroscopy, Shanxi University, Taiyuan 030006, China

[2] Collaborative Innovation Center of Extreme Optics, Shanxi University, Taiyuan 030006, China

*Corresponding author: gangzhao@sxu.edu.cn

**Corresponding author: mwg@sxu.edu.cn

Received April 22, 2023 | Accepted August 15, 2023 | Posted Online January 22, 2024

The dual-mode stabilization scheme has been demonstrated as an efficient way to stabilize laser frequency. In this study, we propose a novel dual-mode stabilization scheme that employs a sizable Fabry–Pérot cavity instead of the microcavity used in previous studies and has enabled higher bandwidth for locking. The results demonstrate a 30-fold reduction in laser frequency drift, with frequency instability below 169 kHz for integration time exceeding 1 h and a minimum value of 33.8 kHz at 54 min. Further improvement could be achieved by optimizing the phase locking. This scheme has potential for use in precision spectroscopic measurement.

Keyword: dual-mode stabilization; laser frequency locking; single-sideband modulation.
DOI: 10.3788/COL202422.011401

1. Introduction

The frequency-stable laser is a powerful tool for high-precision spectroscopy[1–3], optical atomic clocks[4–6], quantum communication[7,8], and gravitational wave detection[9,10]. To achieve frequency stabilization, various approaches have been proposed. The most common method is to lock a laser to a molecular or atomic transition, since the transition frequency is unique and invariant[11–15]. To improve the locking performance, sub-Doppler schemes[16–18], such as saturation absorption, multi-photon absorption, or ultracold molecular spectroscopy, are preferred. These techniques can provide better spectral resolution, leading to stabler locking. By locking a laser to a specific transition, the laser frequency can be precisely controlled and stabilized, enabling high-precision measurements and applications.

Another method is to use an ultrastable optical cavity to purify the laser frequency[19–23]. In addition to the cavity finesse, the consistency of the cavity length plays a dominant role in laser performance.

Passive strategies, such as cryogenic monocrystalline silicon[24–29] and multiple-layer isolation from ambient heat and vibration[30,31], have been introduced to stabilize the cavity length and the free spectral range (FSR). The fractional frequency instability beyond 10^{-18} for integration time of dozens of seconds has been demonstrated. Nevertheless, the drift of the laser frequency is still observable with longer integration time, attributed to the residual influence from ambient conditions.

Active stabilization of the cavity length is another approach. For example, one cavity mode can be locked to a HeNe laser to stabilize the laser frequency at the infrared region[32]. The laser frequency drift of hundreds of kilohertz at the infrared region has been demonstrated. This requires a cavity mirror with a dichroic dielectric coating. Dual-mode stabilization with a whispering-gallery mode cavity has also been proposed[33,34], where two external cavity diode lasers (ECDLs) are locked to two cavity modes, respectively. The beat note between the two laser frequencies is measured and stabilized to an external radio frequency (RF) by actively controlling the temperature of the cavity and the cavity length[35,36]. However, the bandwidth of the control is limited to the hertz level, which cannot compensate for higher frequency noise. Additionally, this method is only suitable for microcavities, which are trivial to control their temperature.

In this paper, a new type of dual-mode stabilization is proposed. A sizable Fabry–Pérot cavity with length of 40 cm is

utilized. The cavity length and the FSR could be feedback controlled by detuning a piezoelectric transducer (PZT) attached to one cavity mirror. This allows a high bandwidth of the control, which is expected to improve the stability of the laser frequency. In addition, a fiber laser is used as the first laser, and a single-sideband modulator (SSM) is used to shift the laser frequency and generate the second laser. By using the same source for both lasers, the common part in their locking deviation is eliminated during the beating process. Therefore, better phase locking should be desired. The paper presents the experimental principle, followed by a detailed description of the experimental setup and procedure. Finally, the measurement results are analyzed to demonstrate the effectiveness of the proposed dual-mode stabilization technique.

2. Experimental Principle

For an optical cavity, the frequency of the nth longitudinal mode of the cavity f_n could be expressed as

$$f_n = nf_{\mathrm{FSR}} + \Delta f, \tag{1}$$

where f_{FSR} is the cavity FSR, i.e., the frequency separation between adjacent cavity resonant modes. Δf represents the offset frequency, introduced by the phase shift of the cavity mirror, and it could be considered as constant for a given laser frequency range[34,37]. When the FSR is stabilized, the mode frequency is effectively "frozen," since it is determined by the cavity length and the FSR. This enables precise control and stabilization of the laser frequency if the laser is locked to an external cavity.

The challenge in cavity-based stabilization lies in accurately measuring and stabilizing the cavity FSR. The proposed scheme of the paper is illustrated in Fig. 1. Two lasers are incident into the cavity and locked to their corresponding cavity modes, respectively. In the frequency domain, the two laser frequencies (represented by two red arrows) coincide with the respective teeth of the cavity mode comb (with orders of n_1 and n_2, respectively). The beat note between the two laser frequencies is equal to a multiple of the cavity FSR, i.e., $(n_1 - n_2) \cdot \mathrm{FSR}$. The beat note as well as the FSR can be acquired by a photodetector and then phase-locked to an external RF by detuning the cavity length. Moreover, it is crucial to emphasize that the beat note, as the error signal, includes any noise arising from the fluctuations in the cavity's length. By controlling the cavity length, the FSR can be stabilized, which in turn stabilizes the laser frequency. Overall, the proposed scheme provides a promising approach for achieving frequency stability in optical cavity-based systems.

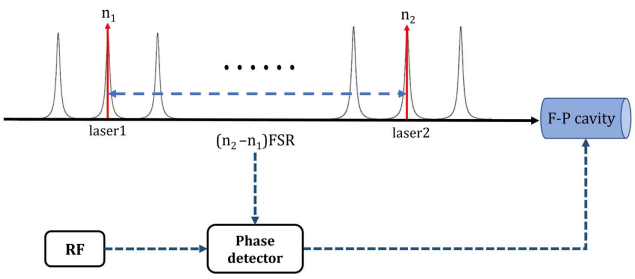

Fig. 1. Principle of the proposed dual-mode stabilization.

3. Experimental Setup

The experimental setup for the proposed dual-mode stabilization is shown in Fig. 2. An erbium-doped fiber laser (EDFL) at 1583 nm with a power of 200 mW is used as the light source. The laser beam goes through a fiber coupled acoustic-optics modulator (f-AOM_1), and then is split into two parts via a fiber splitter, with one part passing through another f-AOM (f-AOM_2) and an electro-optic modulator (f-EOM_1) as the first laser. The laser frequency would be shifted by 80 MHz, i.e., the frequency imposed on the f-AOM_2. The f-EOM_1 is driven by an RF signal at 25.6 MHz to generate modulation sidebands for Pound-Drever-Hall (PDH) locking[38]. The other part passes through a single-sideband modulator (SSM) driven by an RF signal at 3.54 GHz, referred to as f_{vco}, and another EOM, i.e., f-EOM_2, as the second laser. The f-EOM_2 is driven by an RF signal at 19.6 MHz to generate modulation sidebands for the second PDH locking. The two parts are then combined and sent into free space via a fiber-coupled collimator. Before reaching a Fabry–Pérot cavity, the light passes through a matching lens (MML), a half-wave plate ($\lambda/2$), a polarization beam splitter (PBS), and a quarter-wave plate ($\lambda/4$).

The cavity consists of two mirrors with a reflectivity of 99.992% and a cavity finesse of 34,000. The two mirrors are separated by an invar tube with a length of 39.4 cm, corresponding to an FSR of 393 MHz and a cavity mode of 11.6 kHz. The cavity length can be finely detuned using a PZT attached to the rear cavity mirror.

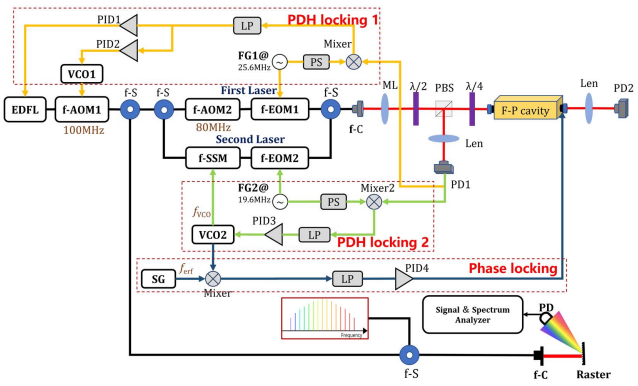

Fig. 2. Schematic diagram of the experimental setup. EDFL, erbium-doped fiber laser; f-AOM, fiber-coupled acoustic optic modulator; f-EOM, fiber-coupled electro-optic modulator; f-S, fiber splitter; f-SSM, fiber-coupled single-sideband modulator; f-C, fiber collimator; MML, mode-matching lens; $\lambda/2$, half-wave plate; $\lambda/4$, quarter-wave plate; PBS, polarization beam splitter; VCO, voltage-controlled oscillator; PD1,2, photodetector; FG, frequency generator; PID, proportional-integral-derivative servo; SG, signal generator; PS, phase shift; LP, low-pass filter.

Two PDH locking processes are employed to lock the two lasers to their corresponding cavity modes, respectively. The cavity reflection is deflected by a PBS and directed towards a reflection detector (PD1). The output of PD1 is demodulated by a reference signal at 25.6 MHz to generate the error signal for the locking of the first laser. The error signal is sent into two home-made proportional-integral-derivative (PID) servos. One servo controls the PZT inside the EDFL and is made up of two cascade integrators and one proportion, which ensures that the gain at low frequencies is sufficient for effective control of the PZT. The other servo controls the driver frequency of the f-AOM_1 so as to broaden the locking bandwidth to 200 kHz. At the same time, the output of PD1 is also demodulated by a reference signal at 19.6 MHz, for locking the second laser to the cavity via the control of the f_{vco}. After this step, the f_{vco} is proportional to the cavity FSR.

To stabilize the cavity FSR, the frequency of the voltage-controlled oscillator (f_{vco}) is mixed with an external RF, and the resulting signal is fed into a PID controller (PID4) to control the stretch of the cavity PZT. This effectively phase-locks the f_{vco} signal to the RF, stabilizing the cavity FSR and the two laser frequencies. Note that all frequency generators in the setup are synchronized to a 10 MHz signal reference generated by a rubidium frequency standard.

The locking performance is analyzed using both the error signals and an optical frequency comb. The former determines the in-loop noise. A part of the laser beam is split and beats with the frequency comb, and then the laser frequency is directly measured to determine the out-loop noise.

4. Experimental Results

The performances of the stabilized lasers are affected by the stability of the two PDH locking processes. Therefore, the performance of the two PDH locking processes used in the experiment has been evaluated by analyzing the error signals. Figures 3(a) and 3(b) are the measured error signals when the laser frequency is unlocked and detuned by scanning the laser frequency. The curve in each panel shows three dispersion structures, with the central one caused by the laser carrier and the two sides caused by the modulation sidebands. The signal-to-noise ratio of 50 for each signal results. The signal's peak and valley coincide with the half-maximum position of the cavity mode, yielding a frequency-to-amplitude conversion rate of 4.3 kHz/V and 5.2 kHz/V, respectively. After locking, the two error signals would be clamped to zero, as illustrated in Figs. 3(c) and 3(d). This indicates that the lasers are successfully locked to their corresponding cavity modes. The error signals could be converted to the frequency deviation, shown on the right coordinate in Figs. 3(c) and 3(d).

To further assess the locking performance, the power spectral density (PSD) of the frequency deviation plotted in Fig. 3 is analyzed and shown in Fig. 4. In each panel of the figure, the PSD in the low frequency region is smaller than 10^{-3} Hz^2/Hz, owing to the high gain in the low frequency region of the PID servos used in the locking processes. When the frequency is larger than 100 Hz, both curves show a relatively flat response with values of 1 Hz^2/Hz and 0.7 Hz^2/Hz, respectively. These results verify that, considering that the cavity has negligible noise in the high-frequency region, the instantaneous linewidths of the two lasers, with observation times shorter than 0.1 ms, are in the range of the hertz level. However, for dual-mode stabilization, this frequency deviation would be inherited via the cavity and amplified by a factor of 500,000, i.e., the ratio of the laser frequency to the voltage-controlled oscillator (VCO) frequency, yielding an absolute laser frequency jittering of around hundreds of kilohertz.

After the two PDH lockings, the cavity length is stabilized with the phase noise of the f_{vco} as the error signal. The measured phase noise between the f_{vco} and the RF reference with unequal frequencies before locking is shown in Fig. 5(a). A sinusoidal signal relative to the frequency difference between the two electrical signals can be observed. And the adjacent peak and valley of the signal indicate a phase difference of π, resulting in the phase noise to amplitude noise ratio of 5.2 rad/V. Figure 5(b) displays the phase noise with locking, which appears as a relatively flat signal, indicating tight locking between the two frequencies with a phase noise of around 0.124 rad. Figure 5(c) depicts the PSD of the frequency deviation with locking retrieved from the phase

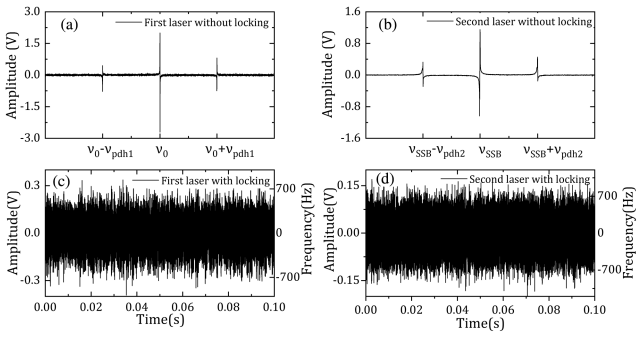

Fig. 3. Error signals for the two PDH locking processes. (a) Without and (c) with locking for the first laser; (b) without and (d) with locking for the second laser.

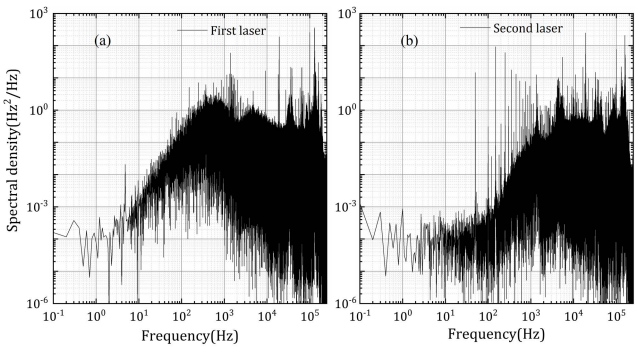

Fig. 4. PSD of the frequency deviation for (a) the first laser and (b) the second laser.

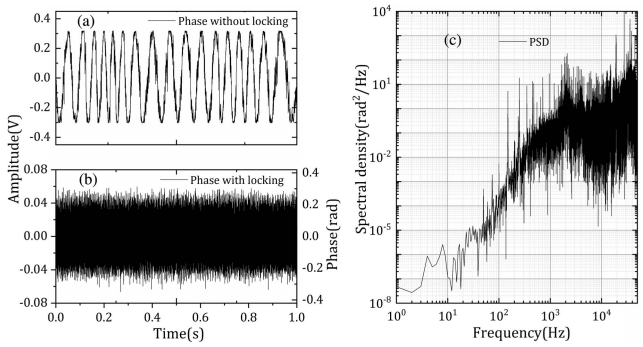

Fig. 5. Locking performance for the phase locking: the phase noise (a) without and (b) with locking; (c) the PSD result of the frequency deviation retrieved from the phase noise.

noise in Fig. 5(b). The PSD value remains constant at 5 Hz^2/Hz for frequencies above 1 kHz, leading to an absolute laser frequency jittering of approximately 1 MHz.

Finally, the absolute laser frequency has been measured by recording the beating frequency between the laser and a frequency comb with the aid of a spectrum analyzer. The result is presented in Fig. 6. Figures 6(a) and 6(b)depict the result without and with phase locking, respectively. To facilitate the comparison, the first datum in each figure is set to 0. It is evident that without phase locking, the laser frequency drifts monotonically due to the instability of the cavity length, which is primarily influenced by ambient environmental variation. In this scenario, the drift exceeds 15 MHz within 10 min. However, with phase locking, the drift is significantly reduced to 2.5 MHz over a period of 110 min, since the drift of the cavity length is compensated by the locking. The corresponding Allan deviations[39] are illustrated in Fig. 6(c), with the black curve representing the data with locking and the blue curve representing the data without locking. It is clear to see that, without locking, when the integration time is longer than 4 s, the Allan deviation increases with a slope of $\sqrt{\tau}$, where τ is the integration time. This means the system is likely dominated by Brownian noise, while, with locking, the drift is suppressed and the suppression ratio could reach 30 at an integration time of 1000 s. The optical

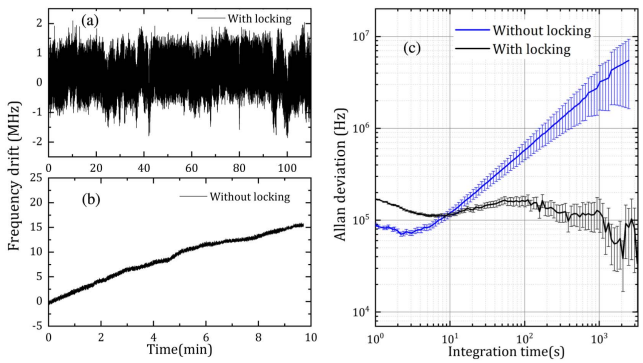

Fig. 6. Laser frequency stability evaluated by the frequency comb: the long-term laser frequency (a) with and (b) without phase locking and (c) their Allan deviation.

frequency instability remains below 169 kHz with the integration time longer than 1 h and reaches its minimum value of 33.8 kHz at the integration time of 54 min. These results confirm that the proposed dual-mode stabilization effectively stabilizes the laser frequency. It is worth noting that the short-term behavior of the laser frequency gets worse owing to the phase locking. The value range is around 2 MHz, and the standard deviation is 89 kHz, with the former being consistent with the frequency jittering introduced by the phase locking of the f_{vco}. In addition, the long-term stability of the locking is believed to be primarily influenced by the drift of the locking offset, which is sensitive to temperature variations.

5. Conclusion and Perspectives

In this paper, we propose a novel dual-mode stabilization scheme to stabilize laser frequency. The scheme utilizes a fiber laser and a single sideband modulator to generate two lasers with different frequencies, which are then locked to their corresponding cavity modes via two PDH lockings. A substantial Fabry–Pérot cavity, instead of the previous employed microcavity, is used. And the cavity length is stabilized by phase locking of the beat note of the two lasers to an RF. Then, the laser frequency could be detuned by varying the RF. To evaluate the locking performance, we measure the error signals for the three locking processes, which indicate the frequency deviation of the lockings. The results show all of the in-loop locking noise in the short term is smaller than 10 Hz^2/Hz, demonstrating that tight lockings have been achieved. Using a frequency comb to analyze the out-loop noise, we found that the drift of the absolute optical frequency is restricted by a factor of 30 by the locking. The optical frequency instability remains below 169 kHz with an integration time longer than 1 h. However, this scheme enlarges the white noise at the laser frequency, owing to the relatively inferior phase locking. Further improvement can be achieved by optimizing the phase locking. This technology is affordable and has the potential to be utilized in applications that only require a laser with a single stable frequency, such as differential absorption lidar (DIAL).

Acknowledgements

This work was supported by the National Key R&D Program of China (No. 2022YFC3700329), the National Natural Science Foundation of China (Nos. 61905134, 61905136, and 62175139), the Shanxi Province Science and Technology Activities for Returned Overseas Researcher (No. 20220001), and the Scientific and Technological Innovation Programs of Higher Education Institutions in Shanxi (No. 2019L0062).

References

1. T. Becker, J. Zanthier, A. Y. Nevsky, *et al.*, "High-resolution spectroscopy of a single In^+ ion: progress towards an optical frequency standard," Phys. Rev. A **63**, 051802 (2001).

2. K. Döringshoff, I. Ernsting, R. H. Rinkleff, *et al.*, "Low-noise, tunable diode laser for ultra-high-resolution spectroscopy," Opt. Lett. **32**, 2876 (2007).
3. S. Borri, M. Siciliani de Cumis, G. Insero, *et al.*, "Tunable microcavity-stabilized quantum cascade laser for mid-IR high-resolution spectroscopy and sensing," Sensors **16**, 238 (2016).
4. A. D. Ludlow, T. Zelevinsky, G. K. Campbell, *et al.*, "Sr lattice clock at 1×10^{-16} fractional uncertainty by remote optical evaluation with a Ca clock," Science **319**, 1805 (2008).
5. A. D. Ludlow, M. M. Boyd, J. Ye, *et al.*, "Optical atomic clocks," Rev. Mod. Phys. **87**, 637 (2015).
6. T. L. Nicholson, S. L. Campbell, R. B. Hutson, *et al.*, "Systematic evaluation of an atomic clock at 2×10^{-18} total uncertainty," Nat. Commun. **6**, 6896 (2015).
7. M. Afzelius, I. Usmani, A. Amari, *et al.*, "Demonstration of atomic frequency comb memory for light with spin-wave storage," Phys. Rev. Lett. **104**, 040503 (2010).
8. E. Togan, Y. Chu, A. S. Trifonov, *et al.*, "Quantum entanglement between an optical photon and a solid-state spin qubit," Nature **466**, 730 (2010).
9. P. W. Graham, J. M. Hogan, M. A. Kasevich, *et al.*, "New method for gravitational wave detection with atomic sensors," Phys. Rev. Lett. **110**, 171102 (2013).
10. C. Cahillane, G. L. Mansell, D. Sigg, *et al.*, "Laser frequency noise in next generation gravitational-wave detectors," Opt. Express **29**, 42144 (2021).
11. B. Chéron, H. Gilles, J. Hamel, *et al.*, "Laser frequency stabilization using Zeeman effect," J. Phys. III France **4**, 401 (1994).
12. K. L. Corwin, Z.-T. Lu, C. F. Hand, *et al.*, "Frequency-stabilized diode laser with the Zeeman shift in an atomic vapor," Appl. Opt. **37**, 3295 (1998).
13. W. Ma, L. Dong, W. Yin, *et al.*, "Frequency stabilization of diode laser to 1.637 μm based on the methane absorption line," Chin. Opt. Lett. **2**, 486 (2004).
14. Y. Han, S. Guo, J. Wang, *et al.*, "Efficient frequency doubling of a telecom 1560 nm laser in a waveguide and frequency stabilization to Rb D_2 line," Chin. Opt. Lett. **12**, 121401 (2014).
15. P. Chang, H. Shi, J. Miao, *et al.*, "Frequency-stabilized Faraday laser with 10^{-14} short-term instability for atomic clocks," Appl. Phys. Lett. **120**, 141102 (2022).
16. A. Bruner, A. Arie, M. A. Arbore, *et al.*, "Frequency stabilization of a diode laser at 1540 nm by locking to sub-Doppler lines of potassium at 770 nm," Appl. Opt. **37**, 1049 (1998).
17. C. Svelto, F. Ferrario, F. F. A. Arie, *et al.*, "Frequency stabilization of a novel 1.5-μm Er-Yb bulk laser to a ^{39}K sub-Doppler line at 770.1 nm," IEEE J. Quantum Electron. **37**, 505 (2001).
18. C. Affolderbach, A. Ch, S. C. Stefka, *et al.*, "Frequency stability comparison of diode lasers locked to Doppler and sub-Doppler resonances," Proc. SPIE **5449**, 396 (2004).
19. G. Mueller, P. McNamara, I. Thorpe, *et al.*, "Laser frequency stabilization for LISA," https://ntrs.nasa.gov/api/citations/20060012084/downloads/20060012084.pdf (2005).
20. A. D. Ludlow, X. Huang, M. Notcutt, *et al.*, "Compact, thermal-noise-limited optical cavity for diode laser stabilization at 1×10^{-15}," Opt. Lett. **32**, 641 (2007).
21. A. Didier, J. Millo, C. Lacroûte, *et al.*, "Design of an ultra-compact reference ULE cavity," J. Phys. Conf. Ser. **723**, 012029 (2016).
22. J. Bai, J. Wang, J. He, *et al.*, "Electronic sideband locking of a broadly tunable 318.6 nm ultraviolet laser to an ultra-stable optical cavity," J. Opt. **19**, 045501 (2017).
23. N. Zhadnov, K. Kudeyarov, D. Kryuchkov, *et al.*, "Long ULE cavities with relative fractional frequency drift rate below 5×10^{-16}/s for laser frequency stabilization," Bull. Lebedev Phys. Inst. **47**, 257 (2020).
24. J. P. Richard and J. J. Hamilton, "Cryogenic monocrystalline silicon Fabry–Perot cavity for the stabilization of laser frequency," Rev. Sci. Instrum. **62**, 2375 (1991).
25. S. Bize, "Ultrastable silicon Fabry–Pérot cavity," Nat. Photonics **6**, 638 (2012).
26. T. Kessler, C. Hagemann, C. Grebing, *et al.*, "A sub-40-mHz-linewidth laser based on a silicon single-crystal optical cavity," Nat. Photonics **6**, 687 (2012).
27. B. Maréchal, J. Millo, A. Didier, *et al.*, "Toward an ultra-stable laser based on cryogenic silicon cavity," in *Joint Conference of the European Frequency and Time Forum and IEEE International Frequency Control Symposium (EFTF/IFCS)* (2017), p. 773.
28. D. G. Matei, T. Legero, S. Häfner, *et al.*, "1.5 μm lasers with sub-10 mHz linewidth," Phys. Rev. Lett. **118**, 263202 (2017).
29. J. M. Robinson, E. Oelker, W. R. Milner, *et al.*, "Crystalline optical cavity at 4 K with thermal-noise-limited instability and ultralow drift," Optica **6**, 240 (2019).
30. J. Alnis, A. Schliesser, C. Y. Wang, *et al.*, "Thermal-noise-limited crystalline whispering-gallery-mode resonator for laser stabilization," Phys. Rev. A **84**, 011804 (2011).
31. S. A. Webster, M. Oxborrow, and P. Gill, "Subhertz-linewidth Nd:YAG laser," Opt. Lett. **29**, 1497 (2004).
32. A. G. Adam, T. E. Gough, and N. R. Isenor, "CO_2 laser stabilization using an external cavity locked to a reference HeNe laser," Rev. Sci. Instrum. **57**, 6 (1986).
33. A. A. Savchenkov, A. B. Matsko, V. S. Ilchenko, *et al.*, "Whispering-gallery-mode resonators as frequency references. II. Stabilization," J. Opt. Soc. Am. B **24**, 2988 (2007).
34. A. B. Matsko, A. A. Savchenkov, V. S. Ilchenko, *et al.*, "Optical-RF frequency stability transformer," Opt. Lett. **36**, 4527 (2011).
35. D. V. Strekalov, R. J. Thompson, L. M. Baumgartel, *et al.*, "Temperature measurement and stabilization in a birefringent whispering gallery mode resonator," Opt. Express **19**, 14495 (2011).
36. I. Fescenko, J. Alnis, A. Schliesser, *et al.*, "Dual-mode temperature compensation technique for laser stabilization to a crystalline whispering gallery mode resonator," Opt. Express **20**, 19185 (2012).
37. A. B. Matsko, A. A. Savchenkov, N. Yu, *et al.*, "Whispering-gallery-mode resonators as frequency references. I. Fundamental limitations," J. Opt. Soc. Am. B **24**, 1324 (2007).
38. R. W. P. Drever, J. L. Hall, F. V. Kowalski, *et al.*, "Laser phase and frequency stabilization using an optical resonator," Appl. Phys. B **31**, 97 (1983).
39. F. Czerwinski, A. C. Richardson, and L. B. Oddershede, "Quantifying noise in optical tweezers by allan variance," Opt. Express **17**, 13255 (2009).